Journal of Materials Chemistry C

Accepted Manuscript

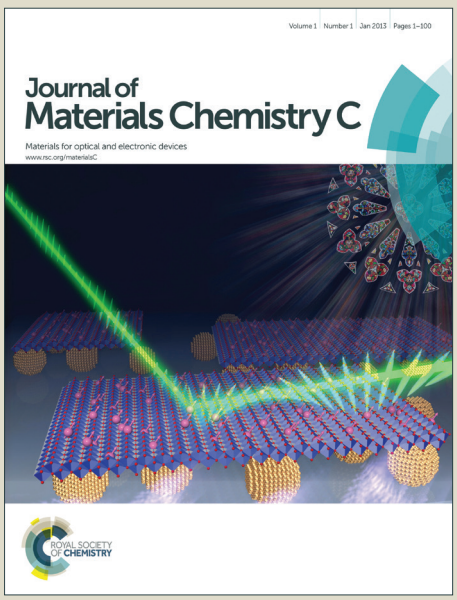

This is an *Accepted Manuscript*, which has been through the Royal Society of Chemistry peer review process and has been accepted for publication.

Accepted Manuscripts are published online shortly after acceptance, before technical editing, formatting and proof reading. Using this free service, authors can make their results available to the community, in citable form, before we publish the edited article. We will replace this *Accepted Manuscript* with the edited and formatted *Advance Article* as soon as it is available.

You can find more information about *Accepted Manuscripts* in the Information for Authors.

Please note that technical editing may introduce minor changes to the text and/or graphics, which may alter content. The journal's standard Terms & Conditions and the Ethical guidelines still apply. In no event shall the Royal Society of Chemistry be held responsible for any errors or omissions in this *Accepted Manuscript* or any consequences arising from the use of any information it contains.

ROYAL SOCIETY OF CHEMISTRY

www.rsc.org/materialsC

Cite this: DOI: 10.1039/c0xx00000x

www.rsc.org/xxxxxx

ARTICLE TYPE

Flexible photodetectors with single-crystalline GaTe nanowires

Gang Yu,[†,‡] Zhe Liu,[†,‡] Xuming Xie,[‡] Xia Ouyang,[‡] and Guozhen Shen*

Received (in XXX, XXX) Xth XXXXXXXXX 20XX, Accepted Xth XXXXXXXXX 20XX
DOI: 10.1039/b000000x

GaTe is an important layer-structured III-VI compound semiconductor with superior optical and electrical properties. In this paper, single-crystalline gallium telluride nanowires were successfully synthesized via a conventional chemical vapor deposition method. Single nanowire field-effect transistor revealed typical p-type semiconductor behavior of the GaTe nanowires, which showed substantial response to light irradiation with broad wavelengths ranging from 350 to 800 nm. Flexible photodetectors on PET substrate were also fabricated with high responsitivity and external quantum efficiency of 20.75 AW^{-1} and 3.96×10^{3}%, respectively. Besides, the flexible photodetectors showed excellent mechanical flexibility and stable electrical properties under different bending states, revealing promising applications in future flexible optoelectronic devices.

Introduction

High-performance flexible microelectronics and macroelectronics utilizing single-crystalline semiconductors as their active materials have been keenly studied in recent years. Flexible devices have potential for various applications, such as electronic devices, displays, sensor chips, therapeutic devices, photodetectors, and the next-generation solar cells.[1-8] These devices have not only retained the bendability, light-weight, and shock-resistant features that plastic materials have to offer but also demonstrated superb performance such as high effective carrier mobility, multigigahertz operation capability, etc. In particular, nano-photodetectors which can convert incident radiation into electrical signals may provide potential applications as binary switches in imaging techniques and light-wave communications, as well as in future memory storage and optoelectronic circuits.[9-14] Benefitting from a large surface-to-volume ratio and a Debye length comparable to their small size, one-dimensional (1D) semiconductor nanostructures are considered as the most promising building blocks for photodetectors with superior sensitivity, high quantum efficiency and fast response speed.[15-17] Compared with the currently hot 2D layered nanostructures, 1D-nanostructures have advantageous in the following three aspects. i) The carriers are confined to a rather small channel zone along 1D-nanostructure rather on a broad surface zone of the 2D layered structure, leading to fabulous electrical characteristics and excellent optoelectronic performance.[18] ii) The crystal growth rate in one dimension at a certain temperature is greatly enhanced with respect to that of the typical 2D layered structure, resulting in structures with a large aspect ratio.[19] iii) The 1D nanostructures for example GaTe NWs offers a coaxial gate-dielectric channel geometry which benefits for further downscaling and electrostatic control.[19] Since Yang et al. reported the first individual nanowire (NW) photodetector in 2002,[15] various types of photodetectors composed of different kinds of 1D semiconducor nanostructures have been fabricated and investigated.[16-27]

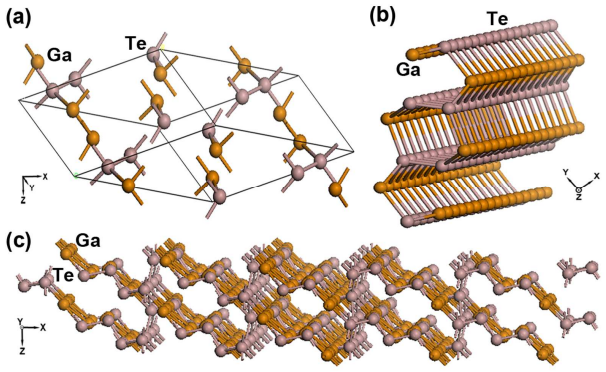

Fig. 1 Structure models of the layer structured GaTe.

Gallium telluride (GaTe) is an important layer-structured III-VI compound semiconductor with each layer consisting of Te-Ga-Ga-Te repeating units stacked along the c-axis (Figure 1). It has a relatively small direct bandgap of *ca.* 1.7 eV at room temperature.[28-29] GaTe are attracting great research interest because of its superior optical and electrical properties for developing electronic and optoelectronic devices. In particular, it holds promising potential for van der Waals epitaxy, Schottky diodes, memory switching, radiation detectors and solar cells.[29-31] However, while the properties of GaTe single crystals, nanoparticles, or two-dimensional (2D) nanosheets have recently been reported in the literature,[31,32] 1D GaTe nanostructures have never been reported, nevertheless the investigation of their corresponding electrical and optical properties.

In this work, well-crystallized single-crystalline GaTe NWs were successfully synthesized via a simple chemical vapor deposition (CVD) method. Single NW field-effect transistor (FET)

Journal of Materials Chemistry C Accepted Manuscript

was fabricated, revealing p-type transistor behaviour with substantial response to light irradiation with different wavelengths ranging from 350 to 800 nm. Flexible photodetectors were also fabricated, exhibiting high responsitivity and external quantum efficiency.

Experimental Section

Single-crystalline GaTe NWs were synthesized in a horizontal quartz tube furnace by using a CVD method. In a typical process, 0.05 g gallium (Ga) sheet and 0.05 g gellurium (Te) powders were mixed and loaded into a ceramic boat. And then the boat was transferred to the center region of the furnace (Thermal Fisher, Linderberg Blue M). (111) Silicon substrates coated with a thin layer of gold nanoparticles about 20 nm were placed at a distance of 12 cm downstream from the center of the furnace to collect the deposited product. Before heating, pure Ar gas was flowed through the system at a rate of 500 sccm for one hour to eliminate oxygen in the reaction system and then maintained at a rate of 150 sccm during the following reactions. After purged for one hour, the furnace was heated up to 1030 ^{o}C at a rate of 20 ^{o}C/min and kept at this temperature for two hours under atmospheric pressure. In the NW growing zone, the temperature was estimated to be 800-850 ^{o}C. After reaction, light black products were found deposited on the substrate.

The as-synthesized products were characterized by X-ray diffractometer (X'Pert PRO, PANalytical B.V., the Netherlands) with radiation of a Cu target (Ka, λ = 0.15406 nm). The morphologies of the products were examined by scanning electron microscopy (FEI Sirion 200, 10 KV; JEOL JSM-6700F, 5 kV; FEI Quanta 200, 10 KV) and transmission electron microscopy (TEM, Tecnai G2 F30). The room-temperature photoluminescence (PL) spectrum was obtained with an FP-6500 spectrometer.

To fabricate single GaTe NW devices, the as-prepared NWs were first sonicated into a suspension in ethanol and then spread onto a SiO_2 (500 nm)/p+-Si substrate. Subsequently, conventional photolithography was performed to pattern the source–drain electrodes, followed by thermal deposition of Cr/Au contact pads with a thickness of 5 nm/100 nm. Flexible photodetectors were fabricated via a similar process except that flexible PET substrate was used instead of rigid silicon substrate. The current-voltage (I-V) as well as the current-time (I-T) characteristics of the fabricated devices were measured using a probe station connected to a Keithley 4200-SCS semiconductor characterization system.

Results and discussion

Fig. 2a shows the X-ray diffraction (XRD) pattern of the as-obtained products. All of the diffraction peaks can be readily indexed as GaTe with a monoclinic structure, which is in good accordance with the standard data file (JCPDS No.33-571). No crystalline peaks from other impurities were observed, indicating the high purity of the as-synthesized GaTe products. Room-temperature PL properties of the GaTe products were also investigated, as depicted in Fig. 2b. A strong emission band centered at ~737 nm was observed, corresponding to the direct band gap of GaTe phase, which is in good accordance with previous reported data.[31]

Figs. 3a,b show the typical SEM images of the as-synthesized GaTe products, from which we can see NWs with diameters of about 100-500 nm and lengths of several tens of micrometers were grown on a large scale on the substrate. TEM images in Figs. 3c,d further confirm the formation of GaTe NWs with uniform geometry and smooth surface along the whole length. A high-resolution TEM (HRTEM) image of a single GaTe NW is shown in Fig. 3e. Two sets of lattice fringes are clearly seen with the interplane spacings of 0.37 nm and 0.39 nm, corresponding to the (-420) and (220) planes of monoclinic GaTe phase, respectively. The elemental maps of Ga, Te an individual GaTe NW (Fig. 3f) are displayed in Fig. 3g and Fig. 3h, respectively. It clearly revealed that each element is homogeneously distributed in the NW, further confirming the formation of pure GaTe NWs.

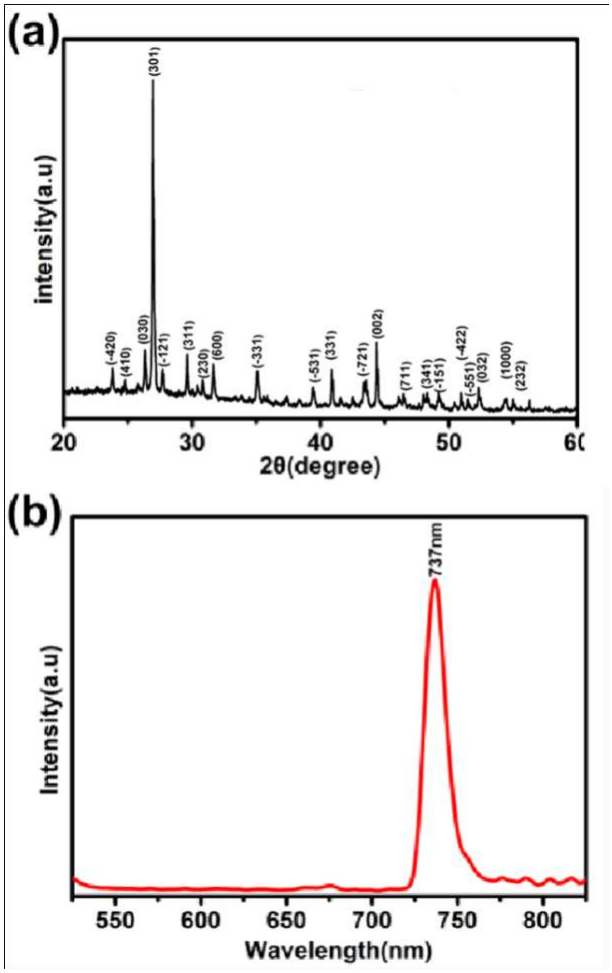

Fig. 2 (a) XRD pattern and (b) room-temperature PL spectrum of the as-synthesized GaTe NWs.

To get information about the electric transport properties of the as-synthesized GaTe NWs, single NW-based FETs were first fabricated using a conventional photolithography process. Fig. 4a shows the drain current (I_{ds}) versus source-drain voltage (V_{ds}) curves of a typical device at different gate voltages. The applied back-gate voltages were set to range from -60 V to 30 V with an average step of 30 V. From the curves, it could be found that the conductance of the device decreased gradually with increased gate voltages, indicating a typical p-type transistor behaviour. Fig. 4b demonstrated the drain current (I_{ds}) versus gate voltage (V_g)

Journal of Materials Chemistry C Accepted Manuscript

This journal is © The Royal Society of Chemistry [year]

characteristics for the GaTe NW FETs at the applied V_{ds} of 5V, which further confirming the p-type semiconductor behaviour of the as-grown GaTe NWs.

With a direct bandgap of *ca.* 1.7 eV, GaTe NWs can in principle detect almost all the visible and ultraviolet lights, which makes them excellent candidates for high performance photodetectors. To evaluate the optoelectronic properties of the as-grown GaTe NWs, single NW-based photodetector was fabricated via a standard lithography procedure. Up inset in Fig. 5a is a schematic illustration of the as-fabricated NW photodetector on silicon dioxide/silicon substrate. The typical SEM image of the device is shown in the lower inset of Fig. 5a.We can see that a single GaTe NW was successfully bridged between the source-drain electrodes with a channel width of about 6 μm. Fig. 5a shows the typical I-V curves obtained when the photodetector is exposed to lights with different wavelengths ranging from 350 to 800 nm with the fixed light intensity of 2.8 mW cm^{-2}. From these curves, it can be seen that the conductance of the GaTe NW obviously depends on the light wavelength .The photocurrent increased gradually as the incident light wavelength changed from 350 to 650 nm and then decreased with the increased light wavelength larger than 650 nm. Since the photocurrent measurements were performed at a constant light intensity, constant photon energy and photon density would be produced per unit time. With larger photon energy, the photon density of the short wavelength light is smaller than the wide wavelength light. Consequently, the photon-induced carrier concentration is smaller than the short wavelength light compared with the large wavelength, so the shorter wavelength light leads to lower photoconductance. What is more, photons of higher energies are preferentially adsorbed at or near the semiconductor surface,[33,34] thus, the decreased photoconductance of the short wavelength light can be ascribed to the decreased carrier density induced by the increased ratio of surface recombination to that of the body part.

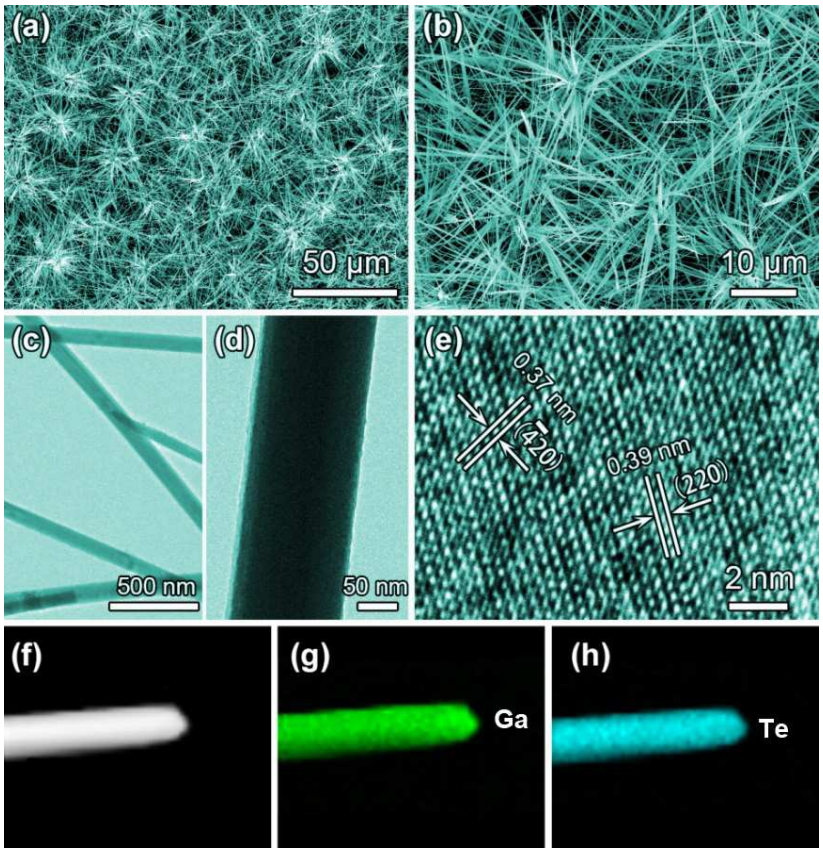

Fig. 3 (a,b) SEM images, (c,d) TEM images, (e) HRTEM image and (f-g) EDS elementral maps of the as-synthesized GaTe NWs, from left to right: EDX elemental mappings of Ga and Te.

Fig. 5b shows the I-V curves of the single GaTe NW photodetector irradiated with light (650 nm) intensities varying from 2.4 mW cm^{-2} to 3.2 mW cm^{-2} stepping by 0.2 mW cm^{-2} at a fixed wavelength of 650 nm. From the curves, we can see that, at a given voltage of 5 V, the conductance increased gradually from 2.09 nS at 2.4 mW cm^{-2} to 2.53 nS at 3.2 mW cm^{-2}. The corresponding dependence of the photocurrent amplitude on the optical power is displayed in Fig. S1. The dependence relation is often expressed by a power law:

$$I=AP^{\theta} \qquad (1)$$

where I is the photocurrent, A is a proportionality constant, P is the light intensity, and θ is an empirical value.[35] Based on the experimental values, the fitting gives an exponential function with θ=0.66.

The spectra responsivity (R_λ) and external quantum efficiency (EQE) are two critical parameters assessing the electrical output per optical input of an optoelectronic device.[36] The responsivity

Journal of Materials Chemistry C Accepted Manuscript

(R_λ) of the present photodetector to 650 nm at 3.2 mW cm^{-2} light is calculated to be 240.3 A W^{-1} by the following equation:

$$R_\lambda = \Delta I / PS \qquad (2)$$

where P is the light intensity irradiated on the nanowire, and S is the effective illuminated area.

The corresponding EQE is calculated to be 4.59×10^4% by the following equation:

$$EQE = hcR_\lambda / e\lambda \qquad (3)$$

where h is the Plank's constant, c is the velocity of light, and e is the elementary electronic charge.

Fig. 5c shows the time response of the device to a pulsed incident light with the wavelength of 650 nm. From the curve, we can see that, when the light intensity is kept constant at 3.2 mW cm^{-2} with a bias voltage of 3V, the photocurrent can be reproducibly switched from the 'ON' state to the 'OFF' state by periodically turning the light on and off. The current of the device mostly exhibited two distinct states and changed very sharply from one state to another state, indicating a fast response speed of the device. The fast response speed is further confirmed by the enlarged portion shown in Fig. 5d. A fast rise time and decay time of the device are found to be about 0.1 s and 0.3 s, respectively.

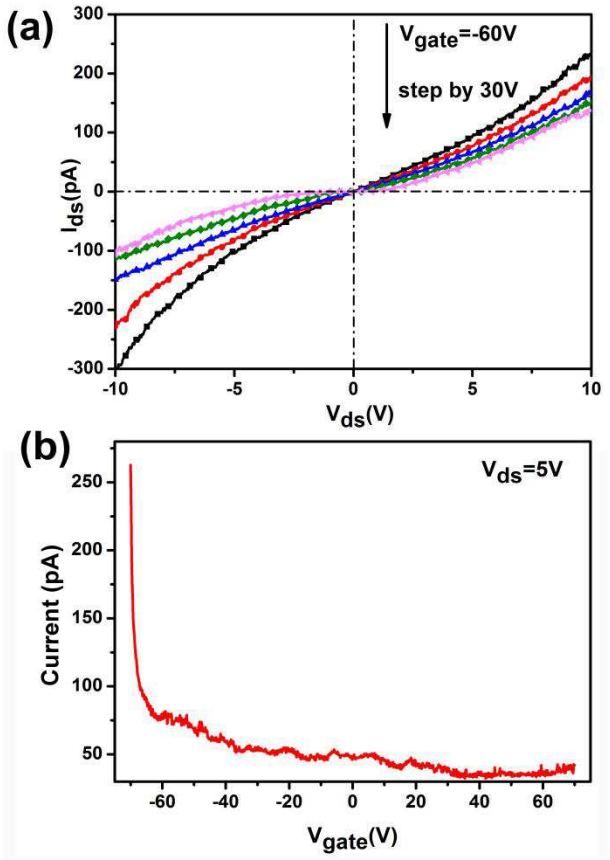

Fig. 4 (a) I_{ds}-V_{ds} curves and (b) I_{ds}-V_g curve of single GaTe NW field-effect transistor.

Fabrication of flexible devices has been one of the hottest topics on optoelectronic research because of their potential applications in various new areas, such as portable device, aerospace science and civil engineering.[37-40] To fabricate flexible GaTe NW based photodetectors, flexible PET substrate was used instead of rigid silicon. Fig. 6a displays a representative schematic illustration of the flexible single GaTe NW photodetector on a flexible PET substrate. Fig. 6b depicts the typical I-V curves obtained when the photodetector is exposed to lights with different wavelengths ranging from 350 to 800 nm with the fixed light intensity of 2.8 mW cm^{-2}. Similar to the rigid photodetector on silicon substrate, the conductance of the flexible device also depends on the light wavelength. When the incident light wavelength changed from 350 to 650 nm, the photocurrent increased gradually and as the light wavelength is larger than 650 nm, the photocurrent decreased accordingly.

The I-V curves of the flexible device at different light intensities (from 2.4 mW cm^{-2} to 3.2 mW cm^{-2} stepping by 0.2 mW cm^{-2}) with fixed light wavelength of 650 nm are shown in Fig. 6c. From these curves, we can calculated that the conductance increased gradually from 107.37 pS at 2.4 mW cm^{-2} to 146.17 pS at 3.2 mW cm^{-2} at the fixed voltage of 5 V. Fig. 6d shows the corresponding dependence of the photocurrent amplitude on the optical power. The dependence relation can also be expressed by equation (1). Based on the experimental values, the fitting gives an exponential function with θ=1.07. The responsivity (R_λ) of the present photodetector to 650 nm at 3.2 mW cm^{-2} light is calculated to be 20.75 A W^{-1} and the corresponding EQE is calculated to be 3.96×10^3%, indicating a high responsivity (R_λ) and EQE for the flexible photodetector as well.

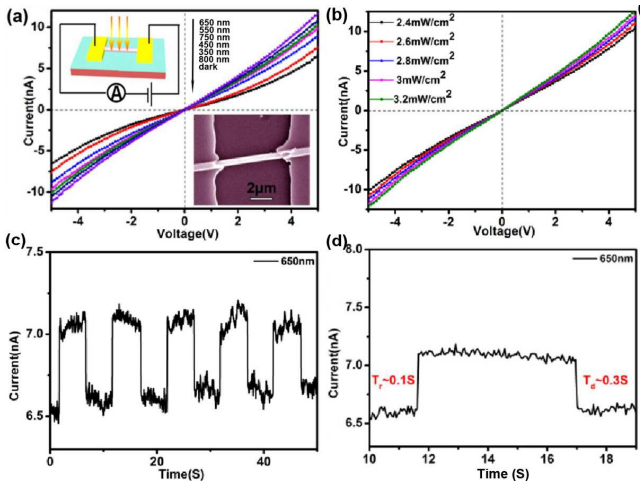

Fig. 5 (a) Spectral response; (b) I-V curves exposed to light of various intensities and (c)Time dependent photocurrent response over 650 nm 3.2 mW cm^{-2} pulsed incident light of the as-synthesized GaTe NWs

The time-dependent photocurrent behaviour of the flexible device to a pulsed incident light with the wavelength of 650 nm was also investigated and the corresponding result was illustrated in Fig 6e. From which we can observe that the photocurrent can be reproducibly switched from the 'ON' state to the 'OFF' state by periodically turning the light on and off with a fixed power density of 3.2 mW cm^{-2} at a bias of 3 V. The current of the flexible device changed sharply from one state to another state, indicating a rapid response speed of the device, similar to the rigid device. Fig. 6f shows the enlarged portion of a single ON-

Journal of Materials Chemistry C Accepted Manuscript

This journal is © The Royal Society of Chemistry [year]

OFF state, which further confirms the rapid response speed with the rise time and decay time of about 0.4 s and 0.5 s, respectively.

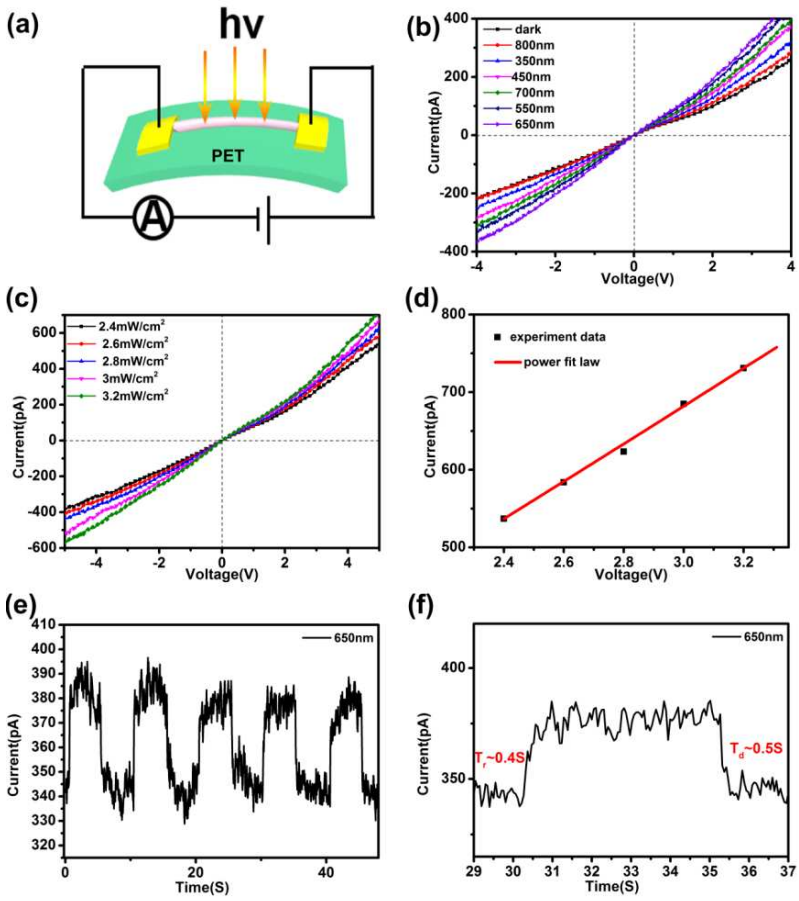

Fig. 6 (a) schematic illustration of a flexible photodetector with a single GaTe NW as the channel on flexible PET substrate. (b) current-voltage curves of the flexible device irradiated by lights with various wavelengths. (c) current-voltage curves of the flexible device irradiated by lights with different light intensities at fixed wavelength of 650 nm. (d) The light intensity dependence of the photocurrent measured at a voltage of 5 V (solid squares). (e,f) Dynamic current-time curves of the flexible device with periodic ON/OFF states to 650 nm light.

The stable electrical properties are important parameters for the practical application of flexible devices. To get information about the electrical stability of our flexible devices, we further examined the current flow through the device at four different curvatures, which are depicted in the upper inset in Fig. 7. The corresponding I-T curves of the flexible device under these states at a fixed voltage of 3 V are shown in Fig. 7. From the curves, we can see that the photocurrent through the flexible device remained nearly unchanged under different bending states, revealing that the conductance of the flexible device is hardly affected by the external bending stress. In order to evaluate the folding endurance, we measured the electrical properties of our flexible device after bending the device for different cycles. As shown in the lower insets in Fig. 7, after bent for 0, 30, 60, 90, 120 and 150 cycles, the corresponding I-V curves match well with each other, further confirming the excellent flexibility and stable electrical properties of the flexible devices. The detailed information for the key parameters of our GaTe NWs as well as some other recently reported III-VI materials is summarized in Table 1, which indicating the prominent performance of our approach.

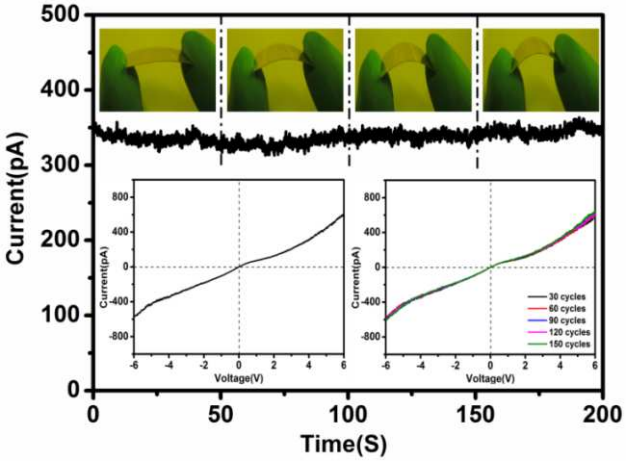

Fig. 7 Current-time plots of the flexible device when bent with various curvatures with a bias of 3V under the same illumination (650 nm, 3.2 $mWcm^{-2}$). The upper section of the picture describes the state of the device and the corresponding photocurrent under different bending radius, namely, 15 mm, 12 mm, 9 mm, 6 mm. The lower insets are the current-voltage curves of the device before after bent for different cycles.

Journal of Materials Chemistry C Accepted Manuscript

Table 1. A summary of the properties for the single III-VI nano-materials based photodetectors.

Nanostructure	*responsivity ($A W^{-1}$)*	*EQE*	*Response time*	*Reference*
GaS nanosheet	19.2	NA	<30 ms	[41]
GaSe nanosheet	2.8	1367%	20 ms	[42]
GaTe nanosheet	274.1	NA	48 ms	[43]
In_2Se_3 NWs	~89 A/W	~22000%	< 0.3 s	[44]
GaTe NWs	240.3	4.59×10^4%	~ 0.3 s	This work

Conclusion

In summary, single-crystalline GaTe nanowires are successfully synthesized via a simple CVD method. Single NW-based FETs exhibited typical p-type transistor behaviour with substantial response to light irradiations with different wavelengths and light intensities. Flexible single GaTe NW-based photodetectors were also fabricated, exhibiting high responsitivity and external quantum efficiency of 20.75 AW^{-1} and 3.96×10^3%, respectively, with excellent mechanical flexibility and stable electrical properties. Our work here may open up the unique possibilities of using GaTe nanowires for the future nano-optoelectronic devices. By applying nanowire assembly techniques, aligned GaTe NW arrays may be obtained to fabricate NW arrays-based photodetectors with optimized performance.

Acknowledgements

This work was supported by the National Natural Science Foundation (91123008, 61377033), the 973 Program of China (No.2011CBA00703), and the Program for New Century Excellent Talents of the University in China (grant no. NCET-11-0179).

Notes and references

State Key Laboratory for Superlattices and Microstructures, Institute of Semiconductors, Chinese Academy of Sciences, Beijing 100083, China. Tel: 86 10 8230 4151; E-mail: gzshen@semi.ac.cn.

† Electronic Supplementary Information (ESI) available: [current-voltage curves of GaTe NW photodetector on silicon substrate at the wavelength of 650 nm with different light intensities, light intensity dependence of the photocurrent measured at the voltage of 5 V, time response of the device on silicon substrate measured under the light with wavelength of 650 nm.]. See DOI: 10.1039/b000000x/

† G. Yu and Z. Liu contribute equally to this work.
‡ G. Yu, Z. Liu, X. M. Xie and X. Ouyang are visiting students from Huazhong University of Science and Technology.

1 X. Liu, Y. Z. Long, L. Liao, X. F. Duan, and Z. Y. Fan, *ACS Nano*, 2012, **6**, 1888.
2 Y. Fang, J. Hou and Y. Fang, *J. Mater. Chem. C*, 2014, **2**, 1178.
3 D. H. Kim, J. H. Ahn, W. M. Choi, H. S. Kim, T. H. Kim, J. Song, Y. Huang, Z. Liu, C. Lu and J. A. Rogers, *Science*, 2008, **320**, 507.
4 Y. Zhan, Y. F. Mei and L. R. Zheng, *J. Mater. Chem. C*, 2014, **2**, 1220.
5 J. Wang, M. S. Gudiksen, X. Duan, Y. Cui and C. M. Lieber, *Science*, 2001, **293**, 1455.
6 B. Liu, J. Zhang, X. F. Wang, G. Chen, D. Chen, C. W Zhou, G. Z. Shen, *Nano Lett.*, 2012, **12**, 3005.
7 Q. Lin, H. Huang, Y. Jing, H. Fu, P. Chang, D. Li, Y. Yao and Z.Y. Fan, *J. Mater. Chem. C*, 2014, **2**, 1233.
8 Z. R. Wang, H. Wang. B. Liu, W. Z. Qiu, J. Zhang, S. H. Ran, H. Tao. Huang, J. Xu, H. W. Han, D. Chen. G. Z. Shen, *ACS Nano*., 2011, **5,** 8412.
9 Z. Liu, T. Luo, B. Liang, G. Chen, G. Yu, X. Xie, D. Chen, G. Z. Shen, *Nano Res.* 2013, **6**, 775.
10 Y. D. Chiou, D. S. Tsai, H. H. Lam, C. H. Chang, K. Y. Lee, Y. S. Huang, *Nanoscale*, 2013, **5**, 8122.
11 G. Chen, B. Liang, X. Liu, Z. Liu, G. Yu, X. Xie, T. Luo, D. Chen, M. Q. Zhu, G. Z. Shen and Z. Fan, *ACS Nano*, 2014, **8**, 787.
12 H. Kobayashi, Y.Koyama, T. Barrett, Y. Hama, C. A. S. Regino, I. S. Shin, B. S. Jang, N. Le, C. H. Paik, P. L. Choyke, Y.Urano, *ACS Nano*., 2007, **1**, 258.
13 G. Chen, Z,. Liu, B. Liang, G. Yu, Z. Xie, H. Huang, B. Liu, X. Wang, D. Chen, M. Q. Zhu and G. Z. Shen, *Adv. Funct. Mater.*, 2013, **21**, 2681.
14 Z. Y. Fan, J. C. Ho, Z. A. Jacobson, H. Razavi, A. Javey, *PNAS*., 2008, **105**, 11066.
15 H. Kind, H. Q. Yan, B. Messer, M. Law, P. D. Yang, *Adv. Mater.*, 2002, **14**, 158.
16 C. Soci, A. Zhang, X. Bao, H. Kim, Y. Lo and D. Wang, *J. Nanosci. Nanotechnol.*, 2010, **10**, 1430.
17 K. Sun, Y. Jing, N. Park, C. Li, Y. Bando and D. Wang, *J. Am. Chem. Soc.*, 2010, **132**, 15465.
18 D. Chen, Z. Liu, B. Liang and G. Z. Shen, *Nanoscale*, 2012, **4**, 3001-3012.
19 C. Thelander, P. Agarwal, S. Brongersma, J. Eymery, L. F. Feiner, A. Forchel, M. Scheffler, W. Riess, B. J. Ohlsson, U. Gösele, and L. Samuelson, *Mater. Today*, 2006, **9**, 28-35.
20 J. J. Wang, F. F. Cao, L. Jiang, Y. G. Guo, W. P. Wu and L. J. Wan, *J. Am. Chem. Soc.*, 2009, **131**, 15602.
21 Y. Wu, X. J. Zhang, H. Pan, W. Deng, X. H. Zhang, X. W. Zhang and J. S. Jie, *Sci. Rep.*, 2013, **3**, 3248.
22 H. Pettersson, J. Tragardh, A. I. Persson, L. Landin, D. Hessman, L. Samuelson, *Nano Lett.*, 2006, **6**, 229.
23 L. Li, E. Auer, M. Y. Liao, X. S. Fang, T.Y. Zhai, U. K. Gautam, A. Lugstein, Y. Koide, Y. Bando, D. Golberg, *Nanoscale*, 2011, **3**, 1120.
24 Y. P. Zhang, X. D. Wang, Y. Wu, J. S. Jie, X. W. Zhang, Y. Xing, H. Wu, B. Zou, X. J. Zhang and X. H. Zhang, *J. Mater. Chem.*, 2012, **23**, 14357.
25 C. Yan, J. Wang, X. Wang, W. Kang, M. Cui, C. Y. Foo and P. S. Lee, *Adv. Mater.*, 2014, **26**, 943.
26 B. Mukherjee, Z. B. Hu, M. R. Zheng, Y. Q. Cai, Y. P. Feng, E. S. Tok and C. H. Sow, *J. Mater. Chem.*, 2012,**22**, 24882.
27 C. S. Lao, M. C. Park, Q. Kuang, Y. L. Deng, A. S. Sood, D. Polla and Z. L. Wang, *J. Am. Chem. Soc.*, 2007, **129**, 12096.
28 M. A. Rahman and A. E. Belal, *J. Phys. Chem. Solids*., 2000, **61**, 925.
29 D. N. Bose and S. Pal, *Phys. Rev. B*, 2001, **63**, 235321.
30 A. Koma and J. Yoshimura, *Surf. Sci*., 1986, **174**, 556.
31 P. Hu, J. Zhang, M. Yoon, W. Feng, P. H. Tan, W. Zheng, J. Liu, X. Wang, J. C. Idrobo, D. B. Geohegan and K. Xiao, *Nano Res.*, 2014, DOI:10.1007/s12274-014-0430-2
32 F. Liu, H. Shimotani, H. Shang, T. Kanagasekaran, V. Zolyomi, N. Drummond, V. I. Fal'ko and K. Tanigaki, *ACS Nano*, 2014, **8**, 752.
33 N. S .Liu, G. J. Fang, W. Zeng, H. Zhou, F. Cheng, Q. Zheng, L. Y. Yuan, X. Zou and X. Z. Zhao, *ACS Appl. Mater.Interfaces*, 2010, **2**, 1973.
34 Y. M. Zhao, J. Y. Zhang, D. Y. Jiang, C. X. Shan, Z. Z. Zhang, B. Yao, D. X. Zhao and D. Z. Shen, *ACS Appl. Mater.Interfaces*, 2009, **1**, 2428.
35 T. Takahashi, P. Nichols, K. Takei, A. C. Ford, A. Jamshidi, M. C. Wu, C. Z. Ning and A. Javey, *Nanotechnology*, 2012, **23**, 045201.
36 L. Li, P. C. Wu, X.S.Fang, T. Y. Zhai, L. Dai, M. Y. Liao, Y. Koide, H. Q. Wang, Y. Bando and D. Golberg, *Adv. Mater*, 2010, **22**, 3161.
37 F. H. Ramirez, J. D. Prades, A. Tarancon, S. Barth, O. Casals, R. J. Diaz, E. Pellicer, J.Rodriguez, M. A. Juli, A. R. Rodriguez, J. R. Morante, S. Mathur, A.Helwig, J. Spannhake and G. Mueller, *Nanotechnology*, 2007, **18**, 195501.
38 A. Marschilok, C. Y. Lee, A. Subramanian, K. J. Taeuchi and E. S. Takeuchi, Energy Environ. Sci., 2011,**4**, 2943-2951

Journal of Materials Chemistry C Accepted Manuscript

This journal is © The Royal Society of Chemistry [year]

39 R. F. Service, *Science*, 2006, **312**,1593.
40 M. C. McAlpine, H. Ahmad, D. W. Wang and J. R. Heath, *Nature Materials*, 2007, **6**, 239.
41 O. Lopez-Sanchez, D. Lembke, M. Kayci, A. Radenovic and A. Kis, *Nat. Nanotechnol.,* 2013, **8**, 497-501.
42 P. A. Hu, Z. Z. Wen, L. F. Wang, P. H. Tan and K. Xiao, *ACS Nano,* 2012, **6**, 5988-5994.
43 P. A. Hu, J. Zhang, M. Yoon, X. F. Qiao, X. Zhang, W. Feng, P. H. Tan, W. Zheng, J. J. Liu, X. N. Wang, J. C. Idrobo, D. B. Geohegan and K. Xiao, *Nano Res.,* 2014, DOI 10.1007/s12274-014-0430-2.
44 T. Y. Zhai, X. S. Fang, M. Y. Liao, X. X. Xu, L. Li, B. D. Liu, Y. Koide, Y. Ma, J. N. Yao, Y. Bando and D. Golberg, *ACS Nano,* 2010, **4**, 1596-1602.

Journal of Materials Chemistry C Accepted Manuscript

Flexible photodetectors with single-crystalline GaTe nanowires

Gang Yu, Zhe Liu, Xuming Xie, Xia Ouyang, and Guozhen Shen*

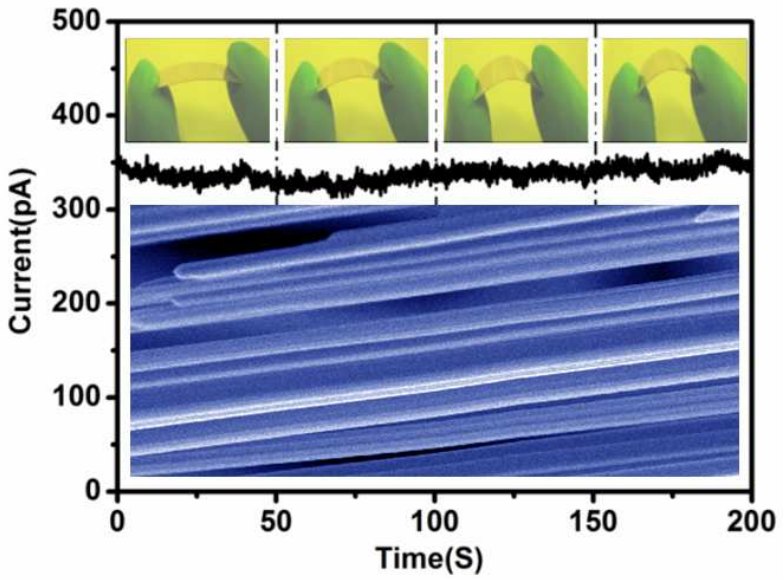

Single-crystalline GaTe nanowires were synthesized for the first time, which are used to fabricate flexible photodetectors with high responsitivity and external quantum efficiency.

Journal of Materials Chemistry C Accepted Manuscript